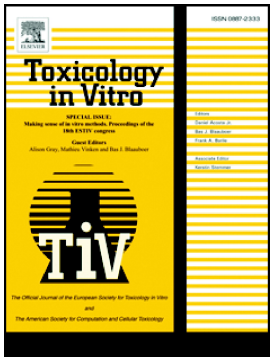

Multifunctional PLGA nanoparticles combining transferrin-targetability and pH-stimuli sensitivity enhanced doxorubicin intracellular delivery and in vitro antineoplastic activity in MDR tumor cells

Laís E. Scheeren, Daniele R. Nogueira-Librelotto, Daniela Mathes, Micheli M. Pillat, Letícia B. Macedo, Montserrat Mitjans, M. Pilar Vinardell, Clarice M.B. Rolim

PII: S0887-2333(21)00117-X

DOI: https://doi.org/10.1016/j.tiv.2021.105192

Reference: TIV 105192

To appear in: *Toxicology in Vitro*

Received date: 2 February 2021

Revised date: 22 April 2021

Accepted date: 9 May 2021

Please cite this article as: L.E. Scheeren, D.R. Nogueira-Librelotto, D. Mathes, et al., Multifunctional PLGA nanoparticles combining transferrin-targetability and pH-stimuli sensitivity enhanced doxorubicin intracellular delivery and in vitro antineoplastic activity in MDR tumor cells, *Toxicology in Vitro* (2021), https://doi.org/10.1016/j.tiv.2021.105192

Multifunctional PLGA nanoparticles combining transferrin-targetability and pH-stimuli sensitivity enhanced doxorubicin intracellular delivery and *in vitro* antineoplastic activity in MDR tumor cells

Laís E. Scheeren[1,2], Daniele R. Nogueira-Librelotto[1,2,*], Daniela Mathes[1], Micheli M. Pillat[2,3], Letícia B. Macedo[1,2], Montserrat Mitjans[4], M. Pilar Vinardell[4] and Clarice M. B. Rolim[1,2,*]

[1] *Departamento de Farmácia Industrial, Universidade Federal de Santa Maria, Av. Roraima 1000, 97105-900, Santa Maria, RS, Brazil*

[2] *Programa de Pós-Graduação em Ciências Farmacêuticas, Universidade Federal de Santa Maria, Av. Roraima 1000, 97105-900, Santa Maria, RS, Brazil*

[3] *Departamento de Microbiologia e Parasitologia, Universidade Federal de Santa Maria, Av. Roraima 1000, 97105-900, Santa Maria, RS, Brazil*

[4] *Departament de Bioquimica i Fisiologia, Facultat de Farmacia i Ciències de l'Alimentació, Universitat de Barcelona, Av. Joan XXIII 27-31, 08028, Barcelona, Spain*

* *Corresponding authors: Phone: +55 55 3220 9548; Fax: +55 55 3220 8248*

E-mail D.R.N.-L.: daniele.rubert@gmail.com

E-mail C.M.B.R: clarice.rolim@ufsm.br

ABSTRACT

Targeted delivery aims to enhance cellular uptake and improve therapeutic outcome with higher disease specificity. The expression of transferrin receptor (TfR) is upregulated on tumor cells, which make the protein Tf and its receptor vastly relevant when applied to targeting strategies. Here, we proposed Tf-decorated pH-sensitive PLGA nanoparticles containing the chemosensitizer poloxamer as a carrier for doxorubicin delivery to tumor cells (Tf-DOX-PLGA-NPs), aiming at alleviating multidrug resistance (MDR). We performed a range of in vitro studies to assess whether targeted NPs have the ability to improve DOX antitumor potential on resistant NCI/ADR-RES cells. All evaluations of the Tf-decorated NPs were performed comparatively to the nontargeted counterparts, aiming to evidence the real role of NP surface functionalization, along with the benefits of pH-sensitivity and poloxamer, in the improvement of antiproliferative activity and reversal of MDR. Tf-DOX-PLGA-NPs induced higher number of apoptotic events and ROS generation, along with cell cycle arrest. Moreover, they were efficiently internalized by NCI/ADR-RES cells, increasing DOX intracellular accumulation, which supports the greater cell killing ability of these targeted NPs with respect to MDR cells. Altogether, these findings supported the effectiveness of the Tf-surface modification of DOX-PLGA-NPs for an improved antiproliferative activity. Therefore, our pH-responsive Tf-inspired NPs are a promising smart drug delivery system to overcome MDR effect at some extent, enhancing the efficacy of DOX antitumor therapy.

Keywords: Smart nanoparticles; Poloxamer; Transferrin; Doxorubicin; Active target delivery; Multidrug resistance; *In vitro* antitumor activity.

1 INTRODUCTION

Doxorubicin (DOX) is an anticancer anthracycline with different mechanisms of action against malignant cells. DOX has high affinity to DNA and can readily bind to its structure. Moreover, it can interact with mitochondria, increase the reactive oxygen species (ROS) production and act as a topoisomerase II poison. Nevertheless, DOX can develop resistance in cancer cells and show some side effects under normal tissues, causing toxicity in healthy cells, especially in cardiomyocytes [1].

According to Minko et al., the mechanism of multidrug resistance (MDR) can be intrinsic or acquired, which are similar and include two major types of resistance named pump and non-pump [2]. A few decades ago, the intrinsic resistance was considered the principal mechanism involved in cancer; however, recent evidence points toward more complex models associated with the acquired mechanism [3]. Previous studies have demonstrated the activity of the triblock copolymers, known as poloxamers, as sensitizers of MDR cells. They have a broad spectrum of action under resistant cells, especially inhibiting Pgp efflux pumps, promoting adenosine triphosphate (ATP) depletion in mitochondria [4], causing apoptosis by reactive oxygen species (ROS) production and cytochrome c release [5] and reducing glutathione (GSH) antioxidant intracellular levels [6].

To improve antineoplastic therapy, several strategies have been investigated. Among them, the drug encapsulation into polymeric nanoparticles (NPs), followed by NP surface decoration with a biomolecule that is able to facilitate an efficient and active drug release into the cancerous cells, is one of the most promising [7]. Transferrin (Tf) is a serum glycoprotein that contains 679 amino acid residues and has a molecular weight of ~ 79 kD. It is responsible for the safe iron transport around the body to supply health growing cells. Tf binds to transferrin receptors (TfR) on the surface membrane of actively dividing cells to release iron-loaded. The level of TfR expression varies according to cell type, being the non-dividing cells those with extremely low levels of TfR expression, whereas rapidly proliferating cells, such as tumor cells, can express up to 100,000 TfR per cell [8]. The TfR ability to uptake molecules via receptor-mediated endocytosis was mentioned elsewhere and, added to its high expression on cancer cells, make the Tf an interesting ligand to target the NPs selectively to tumor cells [9,10].

The poly(lactic-co-glycolic acid) (PLGA) is a biocompatible, biodegradable and safely administrable polymer approved by FDA (Food and Drug Administration) and EMA (European Medicines Agency) for the synthesis of NPs; thus, the best candidate in terms of

performance and design [11]. PLGA intelligent drug delivery systems based on nanotechnology have been extensively studied as remotely triggered strategies for antitumor treatment, including photo-triggered, magnetic field-triggered, ultrasound-triggered, and radiofrequency-triggered cancer therapy [12].

Concerning Tf-conjugated PLGA-NPs containing DOX, studies conducted in different cell models showed interesting results about the higher activity of the Tf-decorated NPs in comparison to NPs without Tf in tumor cells [13–16], as well as in resistant cells [9]. Indeed, to personalize the NP structure with appropriate targets is the focus of many researchers in oncology, including applications in diagnostics, theranostics, medical devices and therapeutics to several cancer types [2,17]. Tf-conjugated red blood cells membrane-coated PLGA NPs encapsulating DOX and the photodynamic agent methylene blue (MB) revealed synergistic action for cancer therapy. The chemo- and photodynamic effects induced by DOX and MB, respectively, resulted in the generation of reactive oxygen species (ROS) and DNA damage, leading to apoptosis mediated cell death of HeLa and MCF-7 tumor cell lines [18]. Synergistic activity of DOX and tetrahydrocurcumin loaded in Tf-modified PEG-PLGA NPs has been also demonstrated, and the enhanced chemotherapeutic potential of this formulation was proved by both *in vitro* and *in vivo* investigations [19].

Previously, we have described the complete preparation and characterization of pH-sensitive Tf-conjugated PLGA-NPs encapsulating DOX (Tf-DOX-PLGA-NPs). It was demonstrated the compatibility of the NPs with human blood components, as well as the noticeable pH-responsive drug release and membranolytic activity profile when the pH value changes from 7.4 to 5.4 [13]. The proposed nanoparticulate system has its polymeric structure firstly modified by the inclusion of a unique and exclusive pH-responsive amino-acid surfactant, the 77KS (N^{α},N^{ε}-dioctanoyl lysine with an inorganic sodium counterion), besides the incorporation of poloxamer as an adjuvant likely able to sensitize MDR cells [13,20–22]. The protein Tf was further conjugated to NP surface to improve the selective targetability of the system. In view of the promising results previously obtained, herein we focus on the *in vitro* study of the potential of these targeted Tf-decorated NPs to overcome MDR of NCI/ADR-RES cells to some extent. The underlying mechanisms of the cytotoxic responses were investigated including the evaluation of the apoptosis rate, ROS formation and cell cycle, along with the assessment of cell uptake, efflux rates, and cell internalization pathways. All evaluations of the Tf-conjugated NPs were performed comparatively to the nontargeted counterparts and free drug, with the aim to evidence the substantial role of DOX encapsulation into the pH-sensitive poloxamer-modified polymeric nanostructure, along with the NP surface

functionalization with Tf, in the improvement of the antiproliferative activity and reversal of MDR. Moreover, the studies were also performed using DOX sensitive MCF-7 tumor cells for comparison purposes.

2 MATERIALS AND METHODS

2.1 *Reagents and chemicals*

Doxorubicin hydrochloride (DOX, state purity 98.32%) was obtained from Zibo Ocean International Trade (Zibo, Shangdong, P.R., China). Dulbecco's Modified Eagle's Medium (DMEM), fetal bovine serum (FBS), phosphate buffered saline (PBS), L-glutamine solution (200 mM), trypsin-EDTA solution (170,000 U/L trypsin and 0.2 g/L EDTA) and penicillin-streptomycin solution (10,000 U/mL penicillin and 10 mg/mL streptomycin) were purchased from Lonza (Verviers, Belgium). Propidium iodide (PI), Annexin V-FITC Apoptosis detection kit, RNAse and 2′,7′-Dichlorofluorescein diacetate were obtained from Sigma-Aldrich (São Paulo, SP, Brazil). The HoechstH33258 staining dye solution was purchased from Fluka (Madrid, Spain). The anionic N^{α},N^{ε}-dioctanoyl lysine-based surfactant with an inorganic sodium counterion (77KS) was synthesized as previously reported [20] and included in the NP structure as the pH-sensitive adjuvant. All other reagents were of analytical grade.

2.2 *Preparation of NPs*

DOX-loaded PLGA nanoparticles (DOX-PLGA-NPs) were prepared by the nanoprecipitation method [23], with some modifications. The full explanation of the preparation procedure was previously described [13]. The surfactant 77KS and the poloxamer were part of the aqueous phase. For NPs surface functionalization, DOX-PLGA-NPs were first activated with EDC/NHS (1-ethyl-3-(3-dimethylaminopropyl) carbodiimide / N-hydroxysuccinimide) and then incubated with Tf, resulting in Tf-DOX-PLGA-NPs. The excess of materials was eliminated by Centrisart® 10 kDa and 100 kDa MWCO centrifugal ultrafiltration unit (Sulpeco).

2.3 *Protein corona study*

The NP suspensions were dispersed in water, DMEM 5% FBS or human plasma, and maintained at 37°C to verify a possible protein aggregation on the surface of the NPs. The DOX concentration in these environments was equivalent to 50 µg/mL (the higher concentration used in the cytotoxicity experiments) and the size and polydispersity index

(PDI) were checked immediately upon dilution, as well as after 24, 48 and 72 h of incubation, by dynamic light scattering using a Malvern Zetasizer ZS (Malvern Instruments, Malvern, UK).

2.4 *Cell lines and culture conditions*

The tumor cell lines HeLa (human epithelial cervical cancer), MCF-7 (human breast cancer) and HepG2 (human hepatocellular carcinoma) were cultured in DMEM (4.5 g/L glucose) supplemented with 10% (v/v) FBS, 2 mM L-glutamine, 100 U/mL penicillin and 100 µg/mL streptomycin. The HeLa and MCF-7 a cell lines were obtained from Eucellbank of Celltec UB (Universitat de Barcelona, Barcelona, Spain). HepG2 cell line was kindly donated by Dr. Miquel Borrás from the Unit of Experimental Toxicology and Ecotoxicology (UTOX) of Scientific Park of Barcelona (Barcelona, Spain). The NCI/ADR-RES (MDR human ovarian cancer cells) were kindly donated by Dr. Antoni Benito from the University of Girona (Spain) and cultured continuously in the same DMEM medium containing 1 µg/mL of DOX [24]. The conditions of the incubator were set at 5% CO2 at 37ºC. Cells with exponential growth phase of 80% confluency were used for experiments.

2.5 *In vitro biocompatibility and antitumor activity assays*

Growth inhibition of the cells was determined using the methyl thiazol tetrazolium (MTT) [25] and neutral red uptake (NRU) assays [26]. All cell lines were seeded into the 96-well cell culture plates and grown overnight under 5% CO2 at 37°C. After this, the treatments DOX-PLGA-NPs, Tf-DOX-PLGA-NPs or free DOX at concentrations ranging from 0.05 to 1.0 µg DOX/mL, diluted in DMEM 5% FBS, were applied and the plates were incubated for 24, 48 and 72 h. For the unloaded-PLGA-NPs, the same dilution rates were used to ensure cell contact with equal concentrations of the NP matrix components. In the second phase of this study, higher concentrations of each treatment, ranging from 2.5 µg/mL to 50 µg/mL, were tested against DOX sensitive and resistant tumor cells, MCF-7 and NCI/ADR-RES, respectively. Then, the treatment-containing medium was removed and replaced by 100 µL of MTT (0.5 mg/mL) or NRU (0.05 mg/mL), both diluted in medium without FBS, following by an additional incubation of 3 h. Thereafter, DMSO or a solution containing 50% ethanol and 1% acetic acid in distilled water was added in which well of the plates from MTT or NRU assay, respectively. Finally, the plates were shacked and the absorbances measured at 550 nm (Tecan microplate reader, Magellan Software V6.6). Viability of the negative control (cells exposed to treatment-free medium) was taken as 100% cell viability [27].

2.6 Cell uptake studies

MCF-7 and NCI/ADR-RES cells (both at 1x105 cells/mL) were seeded in 24-well plates on round cover glasses. After overnight incubation, DOX-PLGA-NPs, Tf-DOX-PLGA-NPs or free DOX were applied to the breast cancer and ovarian cancer resistant cells at concentrations of 2 or 10 µg/mL, respectively. The concentrations were defined based on the results from the cytotoxicity studies mentioned at section 2.5. After 1 and 4 h incubation with the treatments, the cells were rinsed three times with PBS and then staining separately with acridine orange (5 µg/mL) and Hoechst (2 µg/mL), following by incubation under controlled conditions for 15 and 5 minutes, respectively. The cells were washed once again with PBS and then fixed with 4% (v/v) formaldehyde for 15 min at room temperature. Each cover glass was combined with a slide glass and soaked with Prolong ® Gold antifade reagent (Invitrogen) [28]. Once dried, the slides were analyzed on Olympus IX41 fluorescence microscope with a video camera Olympus XC50 and a computer software Olympus cell. B Image Acquisition. The software ImageJ was used to merge the images obtained with the different fluorescent probes.

In order to quantitatively evaluate the cellular uptake of free and nanoencapsulated DOX, MCF-7 and NCI/ADR-RES were cultured in 6-well plates for 24 h at a density of 1.5x105 cells/mL, and then the same concentrations (2 or 10 µg/mL) of each treatment in the respective cell lines were applied, following by 1 and 4 h incubation. Then, the cells were washed three times with PBS and harvested with trypsin, centrifuged and resuspended in PBS until 0.5 mL final suspension. The untreated cells were used as control. Flow cytometry (Sony Spectral Cell Analyzer SA3800) was performed plotting at least 10,000 events per sample and data were analyzed by FlowJo V10.

2.7 Cell internalization pathway

To investigate potential endocytic pathways of DOX-PLGA-NPs, Tf-DOX-PLGA-NPs and free DOX, cell internalization inhibitory tests were carried out on MCF-7 and NCI/ADR-RES cells. The cells were cultured in 6-well plates (1.5x105 cells/mL) and grown overnight. Then, the cells were pre-incubated for 1h with different transport inhibitors in serum-free medium: 1 - sodium azide (NaN3, 1 mg/mL, a cell energy metabolism inhibitor), 2 - chlorpromazine (CPZ, 10 µg/mL, inhibitor of clathrin-mediated endocytosis), 3 - nystatin (NYS, 15 µg/mL, inhibitor of caveolae-mediated endocytosis), 4 - transferrin (Tf, 500 µg/mL, as the inhibitor of the TfR) and 5 - amiloride (AMI, 125 µg/mL, inhibitor of

macropinocytosis). After that, the cells were washed with PBS and treated with NPs or free DOX for 2 h (at 2 or 10 µg/mL, for MCF-7 and NCI/ADR-RES cells, respectively). In addition, to investigate the influence of the temperature on the internalization rate, cells were treated with NPs and free DOX at 4°C, as an energy suppression environment. Finally, the cells were washed, harvested, centrifuged, resuspended to 0.5 mL and the cell fluorescence intensity was quantified by flow cytometry. The concentrations and exposure time used for the inhibitors were determined based on preliminary cytotoxicity studies in each cell line without affecting the cell viability [9,29].

2.8 Intracellular drug retention

The capability of the NPs to increase the DOX accumulation into MCF-7 and NCI/ADR-RES cells was verified by flow cytometry (Sony Spectral Cell Analyzer SA3800). A suspension of $1.5x10^5$ cells/mL was seeded in 6-well plates and after 24 h incubation, the treatments were applied for 4 h (at 2 or 10 µg/mL for MCF-7 and NCI/ADR-RES cells, respectively), then the wells were washed three times with PBS to remove the uninternalized NPs and, subsequently, incubated with fresh DMEM with 10% FBS for 1, 2 and 4 h. At the end of each incubation time, the cells were washed, harvested, centrifuged, resuspended until 0.5 mL final suspension in PBS and analyzed [9].

2.9 Determination of apoptosis rate

The cells were grown to the exponential phase in 60 mm petri dishes (1.5x105 cells/mL) and were then exposed to the treatments. Free DOX, DOX-PLGA-NPs and Tf-DOX-PLGA-NPs were tested at 2 µg/mL or 10 µg/mL in MCF-7 and NCI/ADR-RES, respectively, for 24 h incubation. According to the manufacturer's protocol, cells were trypsinized, centrifuged and resuspended in 0.5 mL of binding buffer 1x. After that, the cells were incubated for 10 minutes with 5 µL of Annexin-V FTIC and 10 µL of PI in the dark. The apoptotic rate was determined by flow cytometry (BD Accuri C6, BD Bioscience) and data were analyzed by FlowJo V10 software [30].

2.10 Cell cycle analysis

Each cell line was cultured in 60 mm petri dishes (1.5x105 cells/mL) and treated with NPs and free DOX at 2 or 10 µg/mL, for MCF-7 and NCI/ADR-RES cells, respectively. After 24 h incubation, the cells were harvested with trypsin/EDTA solution, washed with cold PBS, fixed in ice-cold ethanol (70%) and kept at -20 ºC. Before the analysis in the flow cytometer,

the fixed cells were centrifuged, resuspended in the DNA extraction buffer and incubated for 30 min at 37 ºC. Thereafter, the cells were incubated with the staining solution, prepared with 20 µg/mL PI, 200 µg/mL RNAse and 0.1% Triton X-100 in PBS. The samples were kept in the dark for 1 h and then analyzed by the BD AccuriC6 flow cytometer (BD Bioscience) [30].

2.11 ROS measurement

MCF-7 and NCI/ADR-RES cells were seeded in 60 mm petri dishes at 1.5x105 cells/mL and allowed to grow for 24 h. Free DOX, DOX-PLGA-NPs and Tf-DOX-PLGA-NPs were applied at concentrations of 2 µg/mL to MCF-7 and 10 µg/mL to NCI/ADR-RES cells for 24 h. Then, the cells were washed, harvested and incubated with 0.5 mL of medium containing 5 µM of the ROS-sensitive probe 2′,7′-dichlorodihydrofluorescein diacetate (DCFH-DA) for 20 minutes in the dark and then analyzed by the BD AccuriC6 flow cytometer (BD Bioscience) [31]. The non-treated cells were taken as negative control.

2.12 Statistical methods

The results were shown as average value with standard error (SE). Significance tests were conducted by SPSS® software (SPSS Inc., Chicago, IL, USA), using a one-way ANOVA test with Tukey's post-hoc tests for multiple comparison. p-value < 0.05 was considered statistically significant.

3 RESULTS

3.1 *Protein corona study*

In order to verify any aggregation of NPs in a biological medium and/or the modification of its surface by the adsorption of biomolecules with the formation of a protein corona, the mean particle size and dispersion of the suspensions in different environments were checked. According to the PDI, the systems remaining monodispersed when in water and DMEM; however, in human plasma the PDI increases up to 0.5 for both NPs. Regarding the mean hydrodynamic size of the NPs, there was an augment when in DMEM, especially for DOX-PLGA-NPs, being in contrast to the results in human plasma, in which the mean diameter was maintained throughout the experiment, with non-significant differences. The results are shown in Table 1.

Table 1. Results of the protein corona study after incubation of NP suspensions with cell culture medium and human plasma up to 72 h. The data are expressed as mean ± standard deviation.

NP suspension	Medium	Time incubation at 37±1°C (h)							
		0		24		48		72	
		Size (nm)	PDI	Size (nm)	PDI	Size (nm)	PDI	Size (nm)	PDI
DOX-PLGA-NPs	Water	92.3±0.7	0.11±0.02	85.1±0.8	0.09±0.01	83.7±1.6	0.11±0.01	82.7±0.6	0.11±0.03
	DMEM 5% FBS	90.3±0.2	0.13±0.01	94.2±2.2	0.18±0.01	106.4±1.4	0.20±0.00	112.4±0.4	0.21±0.01
	Human Plasma	53.0±0.8	0.54±0.01	49.4±0.3	0.55±0.00	54.7±0.4	0.53±0.00	61.0±0.9	0.54±0.00
Tf-DOX-PLGA-NPs	Water	89.2±0.7	0.11±0.01	87.6±0.3	0.11±0.00	89.3±0.6	0.11±0.01	88.3±0.7	0.12±0.02
	DMEM 5% FBS	89.6±0.9	0.10±0.01	89.8±0.5	0.13±0.02	90.5±0.6	0.12±0.01	92.0±0.3	0.12±0.01
	Humana Plasm	74.9±0.9	0.31±0.01	75.1±1.2	0.32±0.01	77.3±2.8	0.38±0.08	69.5±1.8	0.47±0.02

3.2 *In vitro cell biocompatibility studies*

The effects of the unloaded-PLGA-NPs on NCI/ADR-RES, HepG2, HeLa and MCF-7 tumor cell lines were evaluated after 24 h treatment by the MTT assay. As evidenced in Figure 1, the unloaded NPs maintained the cell viability higher than 85% regardless of the concentration. The negligible to slight reduction on cell viability indicated the favorable biocompatibility of the designed system.

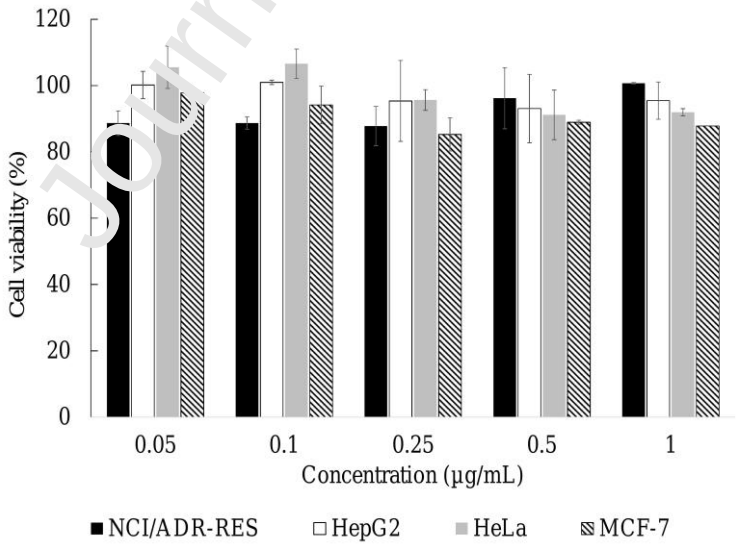

Figure 1. Unloaded-PLGA-NPs in DOX-sensitive and resistant tumor cell lines by MTT assay. Values are expresses as mean ± SD, n = 3.

3.3 *In vitro* antitumor screening

The first antiproliferative studies were performed in different tumor cells treated with DOX-loaded NPs compared to the free drug. Here, due to the DOX-sensitivity of the three cell lines, low drug concentrations ranging from 0.05 to 1 µg/mL were assayed, and the cell viability was measured by MTT and NRU endpoints. As can be seen in Figures S1 and S2, respectively, the NPs clearly affected the cell proliferation in a time-dependent manner, as expected. Both viability assays showed the cytotoxic behavior of the free DOX as well as its higher activity when nanoencapsulated, especially in Tf-conjugated NPs, which markedly reduced the viability up to 25%, 3% and 10% in MCF-7, HeLa and HepG2 cells, respectively, at the highest tested concentration, as detected by the MTT assay (Figure S1). The most expressive statistically significant decreases in cell viability were induced by Tf-DOX-PLGA-NPs in HeLa and HepG2 cell lines, when detected by MTT and NRU assays, respectively ($p < 0.05$).

As the next step of this study and with the aim to verify the ability of Tf-DOX-PLGA-NPs in reverting MDR to some extent, the cytotoxic studies were conducted with NCI/ADR-RES resistant cells, using the standard MTT viability endpoint. NCI/ADR-RES cells are resistant to DOX and, thus, a wider range of DOX concentration was used (2.5 to 50 µg/mL), as higher drug concentrations are needed to achieve a decrease in cell viability. Likewise, by using higher DOX concentrations, it was possible to confirm the resistant pattern of the cell line to non-associated DOX. The same higher concentration range was tested on the MCF-7 cells, which was used as a sensitive cell model for comparison purposes. In Figure 2 is shown that the administration of both targeted and nontargeted DOX-NPs to DOX-sensitive MCF-7 cells displayed similar inhibitory effects to free drug. On the other hand, the NCI/ADR-RES cells showed none or very low response to the treatment with non-associated DOX even after 72 h incubation (at most 36.63% cytotoxicity). DOX-PLGA-NPs were more efficient to kill the resistant MDR cells than the free drug, especially at the highest tested concentrations, 25 and 50 µg/mL, from 48 h. Noteworthy, these phenomena were more remarkable by Tf-DOX-PLGA-NPs, which were even more potent to inhibit the growth of NCI/ADR-RES ($p < 0.05$). For example, 2.5 µg/mL of Tf-decorated NPs started from 70.57% cell viability in 24 h, while free DOX showed 87.57%. This difference becomes even more notable after 48 h of incubation ($p < 0.05$). At 50 µg/mL, free DOX and Tf-DOX-PLGA-NPs displayed 79.49% and 17.87% cell viability, respectively, meaning a ~ 4.5-fold increase in the Tf-NPs cytotoxic potential. After 72 h treatment, the greater antiproliferative effect of Tf-modified NPs was maintained, reaching 14.21% cell viability vs 63.37% of free DOX. Finally, although having

slight cytotoxicity due to a long incubation time, unloaded-NPs exhibited good biocompatibility (at most ~ 20% cytotoxicity in both cell lines).

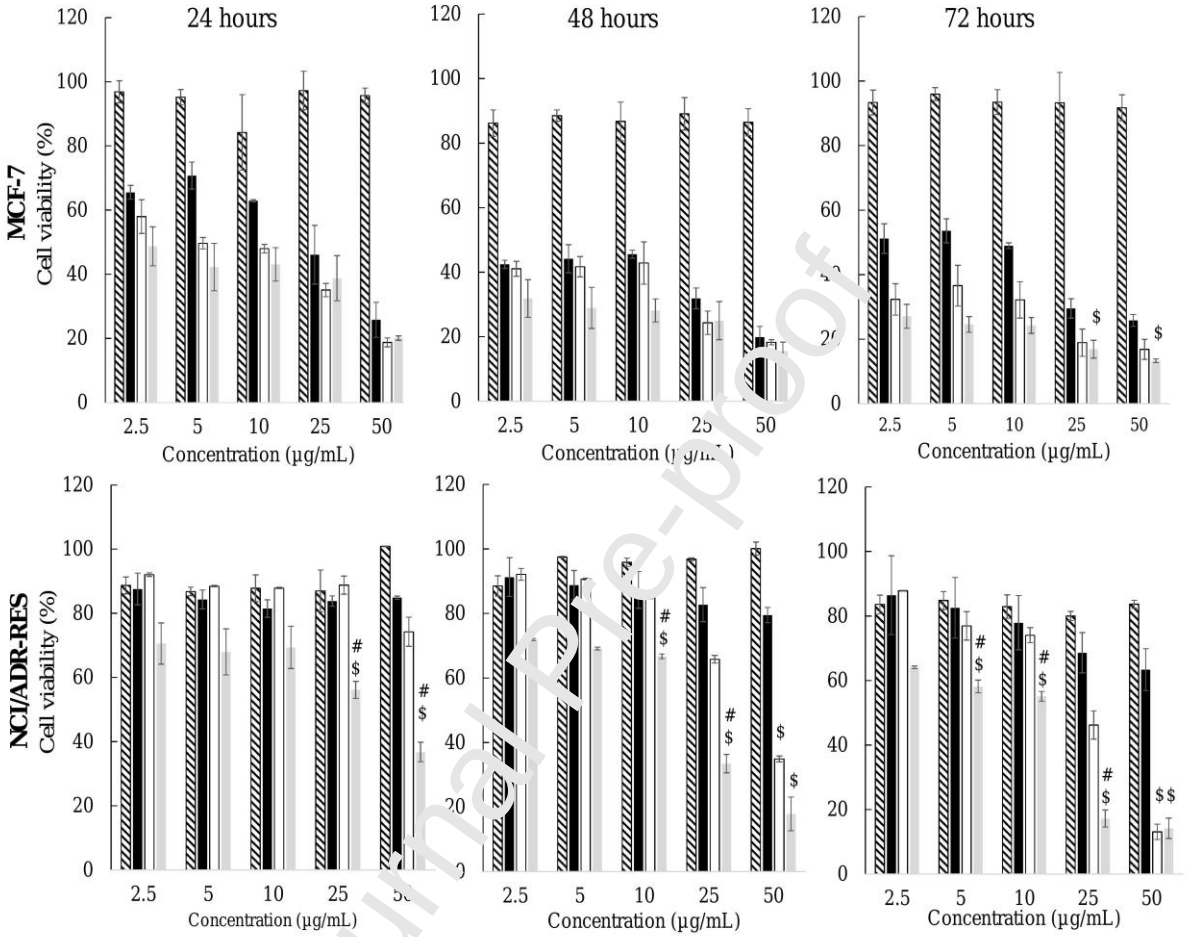

Figure 2. Comparison between MCF-7 and NCI-ADR-RES cell lines by MTT assay, where hatched bars represent unloaded-PLGA-NPs, black bars free DOX, withe bars DOX-PLGA-NPs and gray bars Tf-DOX-PLGA-NPs. Statistical analysis was performed using ANOVA followed by Tukey's multiple comparison test. # is different from DOX-PLGA-NPs and $ is different from free DOX ($p < 0.05$). Values are mean ± SD, n = 3.

3.4 Cell uptake studies

In the cell uptake assessments, as well as in the further experiments performed in this study using flow cytometry, 2 µg/ml and 10 µg/ml DOX concentrations for MCF-7 and NCI/ADR-RES cells, respectively, were chosen because they maintain cell viability close, but higher than 50%, after 24 h incubation. In these experiments, the treatments must not induce excessive cell mortality.

The cellular uptake study via staining the nucleus with Hoechst was confirmed by fluorescence microscopy. The captured images also showed the differences in the internalization and distribution pattern of the non-associated drug, DOX-PLGA-NPs and Tf-DOX-PLGA-NPs when applied to the MCF-7 (Figure 3) and NCI/ADR-RES (Figure 4) cells in a time-dependent manner, besides showing the DOX cell distribution via each treatment. The overlap of red (DOX) and blue (Hoechst) fluorescence signals forming a purple shade indicates that the DOX delivered to the cells via NPs is located in the nucleus with higher intensity in the MCF-7 cells. For the NCI/ADR-RES cell line, the red signal can be seen along the cytoplasm and the cell nucleus. The weakest DOX signal was detected in the free DOX treated group, probably due to the resistant cell profile, while Tf-DOX-PLGA-NPs treated group displayed the strongest purple signal.

Besides, flow cytometry analysis was further performed on sensitive MCF-7 and multidrug resistant NCI/ADR-RES cells to quantitatively study the time-dependent internalization pattern of Tf-DOX-PLGA-NPs, DOX-PLGA-NPs and free drug, with non-treated cells as control (Figure 5). The intrinsic fluorescence intensity of DOX (represented as mean fluorescence intensity) was directly proportional to the internalized drug amount. It was observed a similar pattern for DOX-PLGA-NPs and the non-associated drug, for each cell line. However, significant enhancement in the uptake of Tf-DOX-PLGA-NPs was evidenced in both cell lines at studied timepoints ($p < 0.05$), especially in the MDR cells.

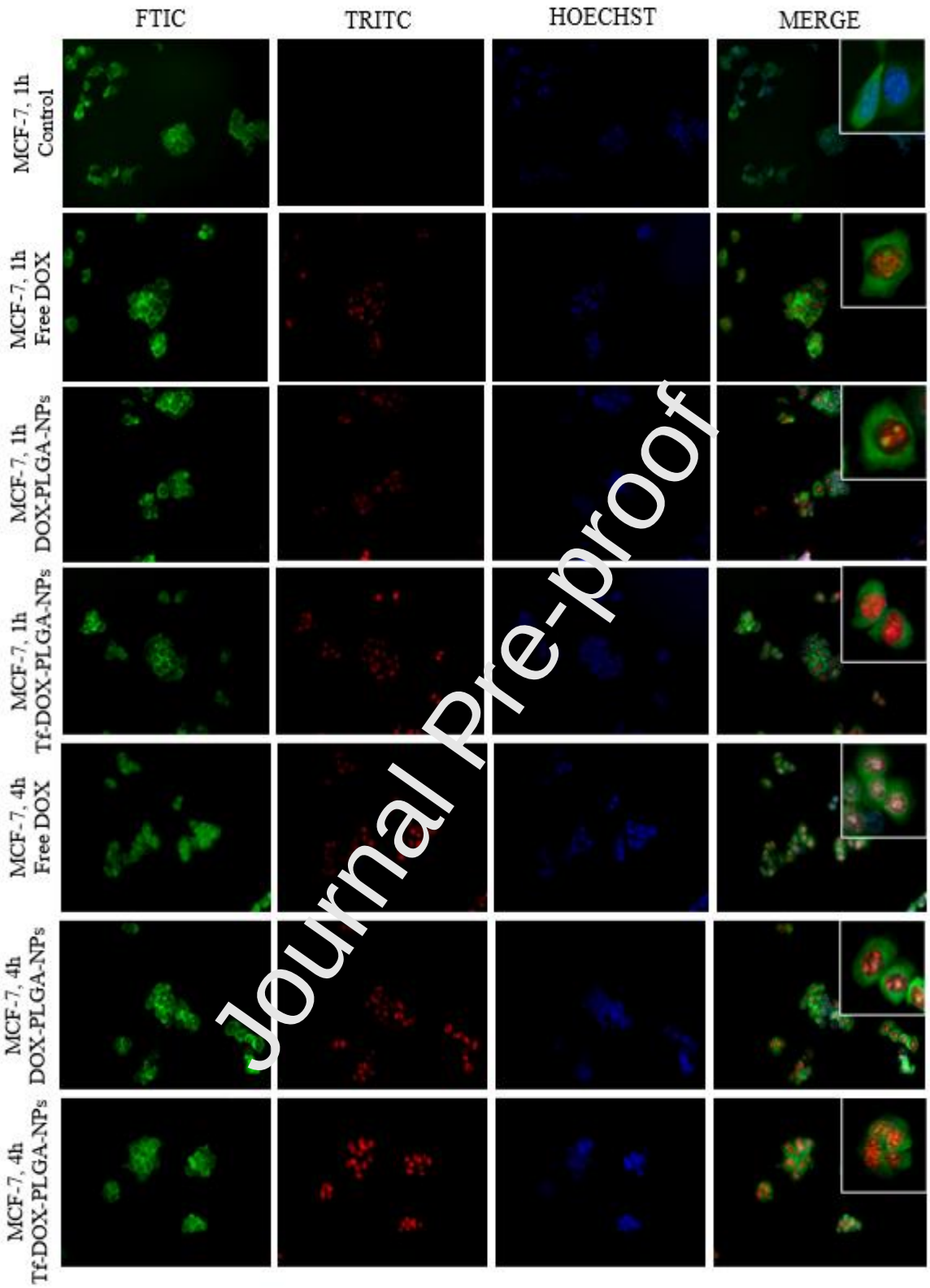

Figure 3. Uptake of free and loaded DOX by MCF-7 (2 µg/mL) cells. Images were captured by fluorescence microscopy following 1 and 4 h incubation.

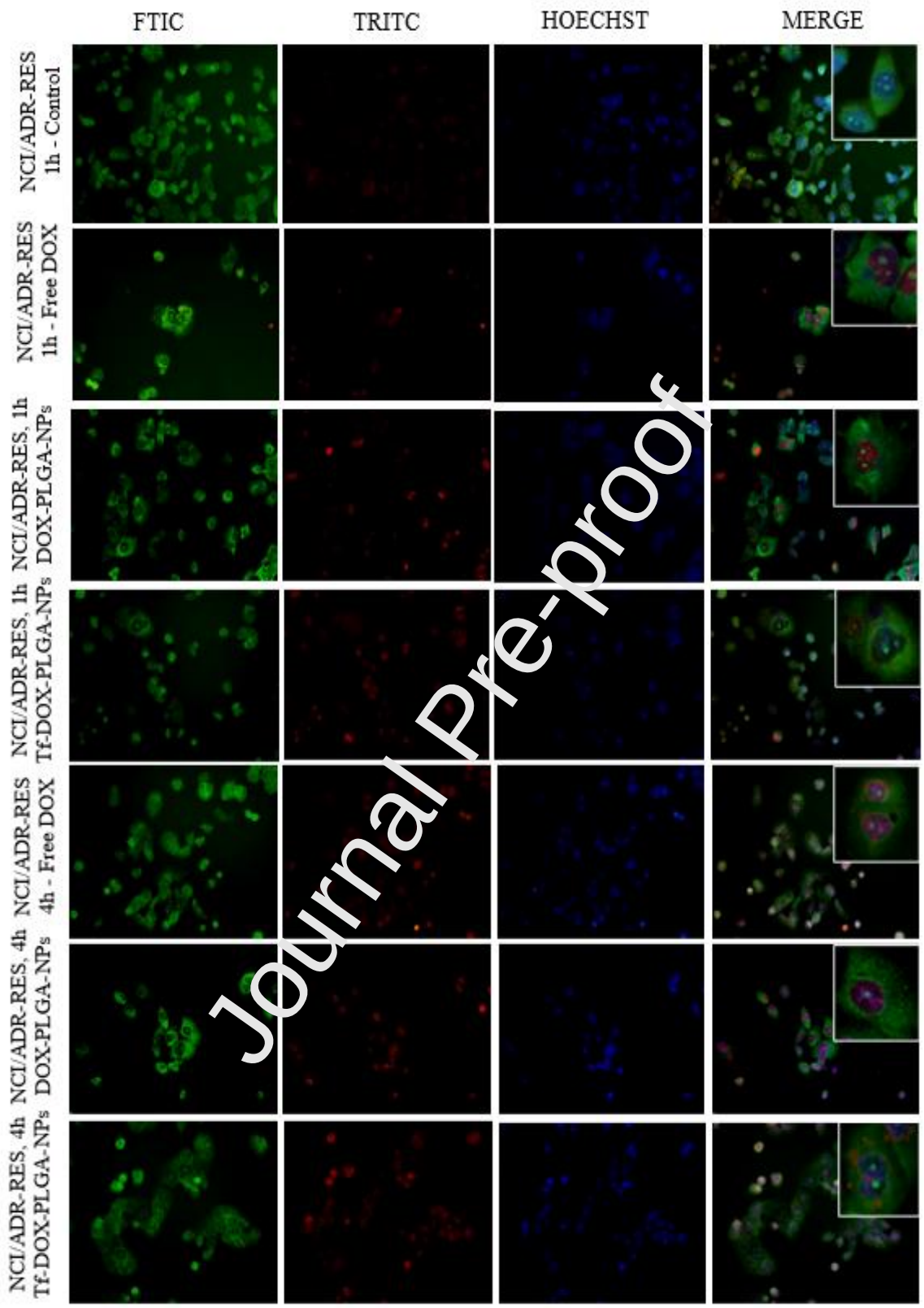

Figure 4. Uptake of free and loaded DOX by NCI/ADR-RES (10 μg/mL) cells. Images were captured by fluorescence microscopy following 1 and 4 h incubation.

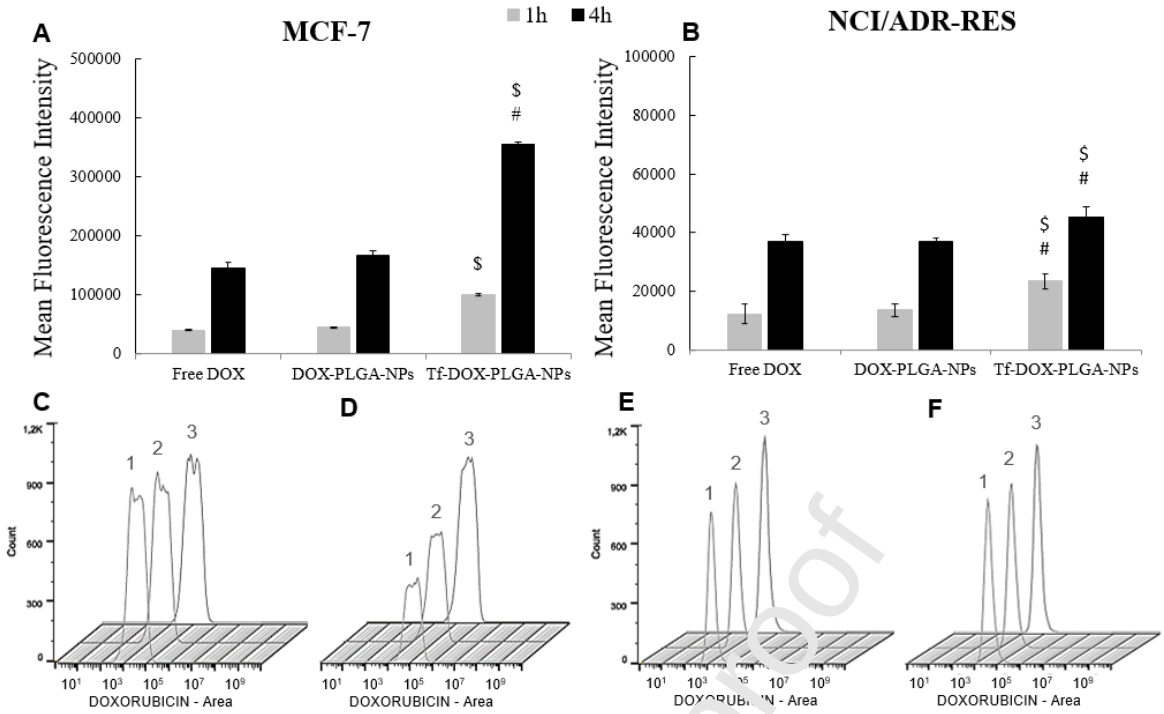

Figure 5. Cell uptake by MCF-7 (A) and NCI/ADR-RES (B) cells of free DOX, DOX-PLGA-NPs and Tf-DOX-PLGA-NPs determined by flow cytometry following 1 and 4 h treatment. Flow cytometry profiles of cellular uptake: (C) at 1 h and (D) at 4 h in MCF-7 cells, and (E) at 1 h and (F) at 4 h in NCI/ADR-RES cells. Legends: (1) free DOX, (2) DOX-PLGA-NPs and (3) Tf-DOX-PLGA-NPs. $^{\$}$ $p < 0.05$ and $^{\#}$ $p < 0.05$ denotes a significant difference from free DOX and DOX-PLGA-NPs, respectively. Values are mean + SD, n = 3.

3.5 Cellular internalization pathway

Internalization mechanisms of the NPs were investigated with specific endocytic inhibitors by flow cytometry in MCF-7 and NCI/ADR-RES cell lines (Figure 6). Compared with Tf-DOX-PLGA-NPs without inhibitors, the DOX cell uptake in MCF-7 cells was slightly inhibited by NaN_3 and Tf, with the intracellular DOX concentration corresponding to 95% and 93%, respectively, of the concentration found in control cells. These findings indicate that the cellular uptake can be mediated by an active energy-dependent process and/or by TfR. In NCI/ADR-RES cells, a 14% inhibition of Tf-DOX-PLGA-NPs internalization was observed after pretreatment with Tf, indicating a possible cellular uptake mediated by TfR. Moreover, it was observed a remarkable reduction of the NP cell internalization when incubated at 4 ºC. No inhibition in the uptake of DOX was found when cells were pretreated with the others tested inhibitors.

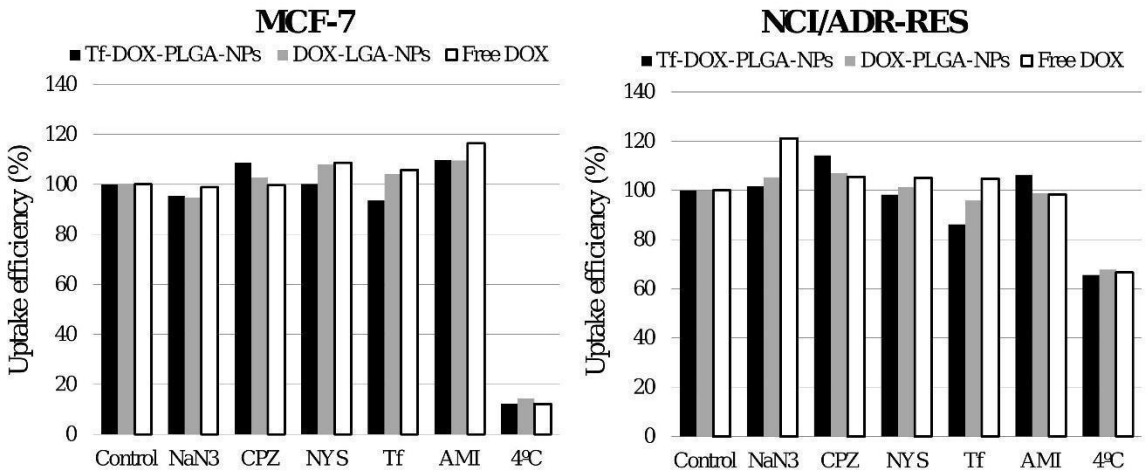

Figure 6. Effect of endocytic inhibitors on cellular uptake in MCF-7 and NCI/ADR-RES cells treated with NPs and free DOX. Cells were incubated with the inhibitor for 1 h prior to DOX formulation treatment for 2 h. The uptake ratio represents the fluorescence intensity in the presence of the inhibitors normalized to control without any inhibitor. NaN3 is sodium azide, CPZ is chlorpromazine, NYS is nystatin, Tf is transferrin and AMI correspond to amiloride.

3.6 Intracellular drug retention

To investigate whether the DOX-loaded-NPs enhance the drug retention inside the cells, flow cytometry was used to measure the DOX intensity. The cells were equally treated during 4 hours, washed and then kept with fresh medium up to 4 h. As can be seen in Figure 7, the mean fluorescence intensity was proportional to the DOX amount remaining inside the cells. The Tf-DOX-PLGA-NPs were the most internalized and were capable of minimizing drug efflux, maintaining a slightly higher level of drug concentration inside the cancer cells.

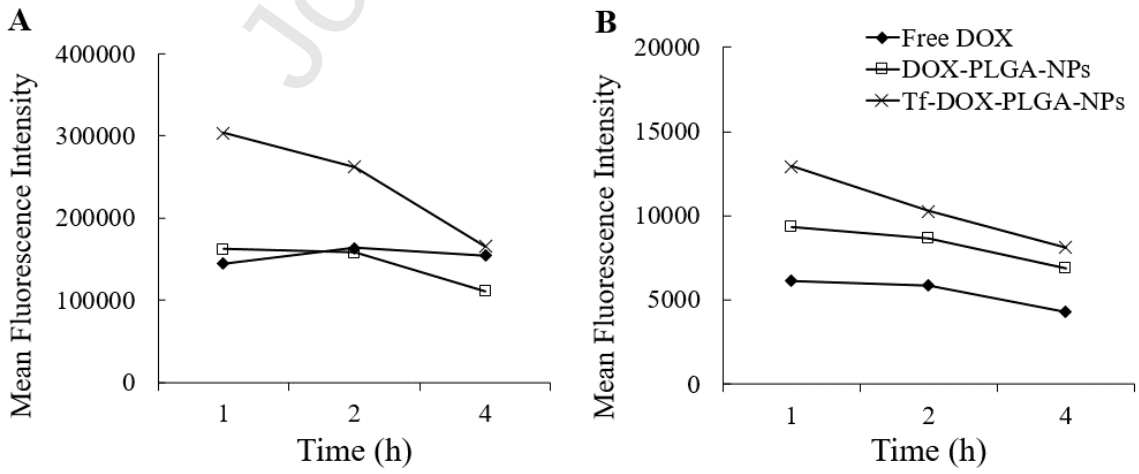

Figure 7. Intracellular retention of the free DOX and DOX-loaded-NPs from MCF-7 (A) and NCI/ADR-RES (B) cells verified by flow cytometry. Cells were incubated for 4 h with each treatment, and then with fresh medium for 1, 2 and 4 h before analysis.

3.7 Apoptosis

In order to determine whether the initial cell death in MCF-7 and MDR cells exposed to free DOX and DOX-loaded NPs could be due to apoptosis, the programed cell death, Annexin V-FTIC/PI assay was carried out and analyzed by flow cytometry. The dual staining Annexin V-FTIC/PI allows to discriminate between unaffected, early apoptotic and late apoptotic/necrotic cells, according the translocation of phosphatidylserine from the inner plasma membrane to the cell surface in the apoptosis stage. Figure 8 shows that the total amount of cell death increased after all DOX treatments in both cell lines. Free DOX was expected to show apoptotic effects and this was actually observed, mainly under sensitive cells. Likewise, DOX-PLGA-NPs and Tf-DOX-PLGA-NPs exhibited similar effects in MCF-7 cells; however, when NCI/ADR-RES cells were treated with Tf-DOX-PLGA-NPs, a substantial increase in the number of apoptotic cells was achieved. Indeed, 32% of the cell population was detected as early apoptotic, which means an approximate 1.5 and 3.0-fold increase in apoptotic response as compared with that caused by DOX-PLGA-NPs and free drug, respectively ($p < 0.05$). Altogether, these results portrayed the role of nanoencapsulation of DOX and the inclusion of Tf to increase the apoptotic-mediated death of MDR cells.

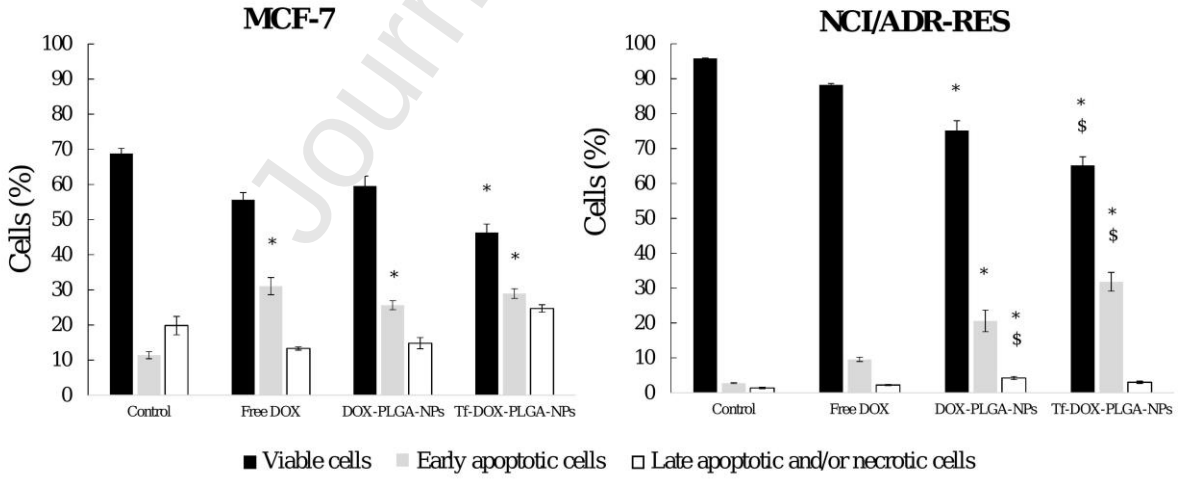

Figure 8. Induction of cell death by free DOX, DOX-PLGA-NPs and Tf-DOX-PLGA-NPs in MCF-7 and NCI/ADR-RES cells. The results are expressed as the percentual of viable, early apoptotic and late apoptotic/necrotic cells after 24 h incubation with each treatment. Statistical analysis was performed using ANOVA followed by Dunnett's or Tukey's multiple comparison test. * $p < 0.05$ and $^{\$}$ $p < 0.05$

denote significant difference from control cells and from free DOX, respectively. Values are mean ± SD, n = 3.

3.8 *Cell cycle analysis*

To further investigate the mechanism underlying the antitumor activity, cell cycle distribution of MCF-7 and NCI/ADR-RES cells treated with free and loaded DOX was assessed by PI staining (Figure 9). For the MCF-7 cells, the results showed that both free DOX and DOX-loaded NPs arrested the cell cycle in G2/M phase. After 24h treatment, the percentual of cells in G2/M phase was ~ 10% in control and increased to 30%, 24% and 45% when treated with free DOX, DOX-PLGA-NPs and Tf-DOX-PLGA-NPs, respectively. The expressive effect of the Tf-conjugated NPs on G2/M phase was accompanied by a suppression of the G0/G1 phase (14% vs 52% in control) and an augment of the S phase (33% vs 30% in control). The NCI/ADR-RES cells had the cell cycle arrested in G2/M phase by the free DOX and DOX-PLGA-NPs (~38% and 42%, respectively) compared to the control group (23%). On the other side, the behavior of the resistant cells when treated with Tf-conjugated NPs was quite different. No cell arrest was observed in G2/M phase, but a slight arrest on the S phase (30% vs 24% in control). Also, it was noted an increase in the percentual of accumulated MDR cells in sub-G1 phase after treatment with Tf-modified NPs.

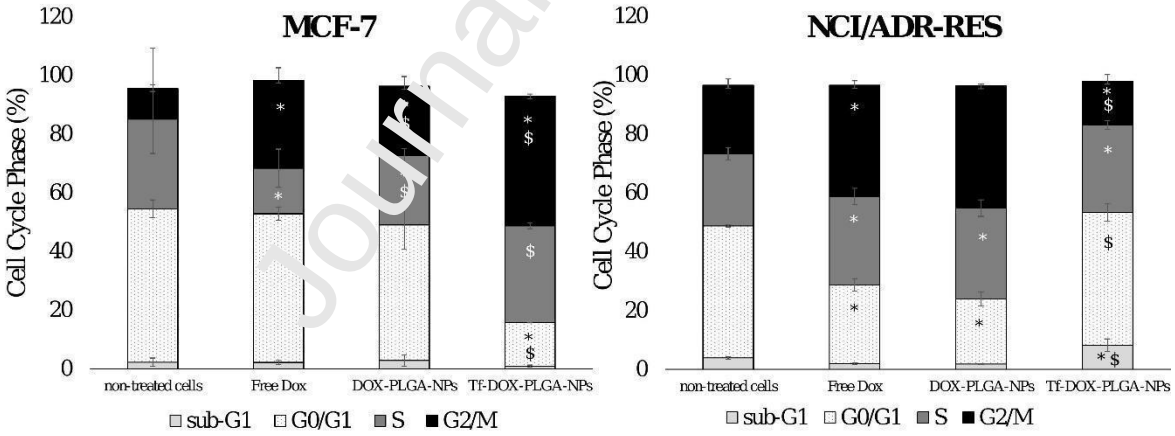

Figure 9. Cell cycle analysis of MCF-7 and NCI/ADR-RES tumor cells following 24 h treatment. The analyses were performed by flow cytometry and the results are expressed as the percentage of cells in each cell cycle phase. Statistical analysis was performed using ANOVA followed by Dunnett's or Tukey's multiple comparison test. * $p < 0.05$ and $^{\$}$ $p < 0.05$ denote significant difference from control cells and from free DOX, respectively. Values are mean ± SD, n = 3.

3.9 ROS measurement

The effect of the different treatments on ROS formation in resistant and sensitive cells was determined by measuring the fluorescent intensity of dichlorofluorescin using flow cytometry. As can be seen at Figure 10, Tf-conjugated NPs showed much higher ROS producing abilities than non-targeted NPs in both sensitive and resistant cells lines. Moreover, ROS produced in cells after treatment with non-associated DOX was found to be only slightly higher than that produced by untreated control cells. Indeed, the ROS levels in MCF-7 sensitive cells increase from 3.75% after free DOX treatment to 47.75 and 86.45% when treated, respectively, with DOX-PLGA-NPs and Tf-DOX-PLGA-NPs ($p < 0.05$). Likewise, the NCI/ADR-RES cells also displayed increased ROS levels after treatment with the NPs. The percentual was lower but not less expressive, increasing from 3.80% with DOX to 29.55% and 50.85% after cell treatment with DOX-PLGA-NPs and Tf-DOX-PLGA-NPs ($p < 0.05$). These results represent a ROS formation at least 7.7-fold higher by NPs compared to the free DOX.

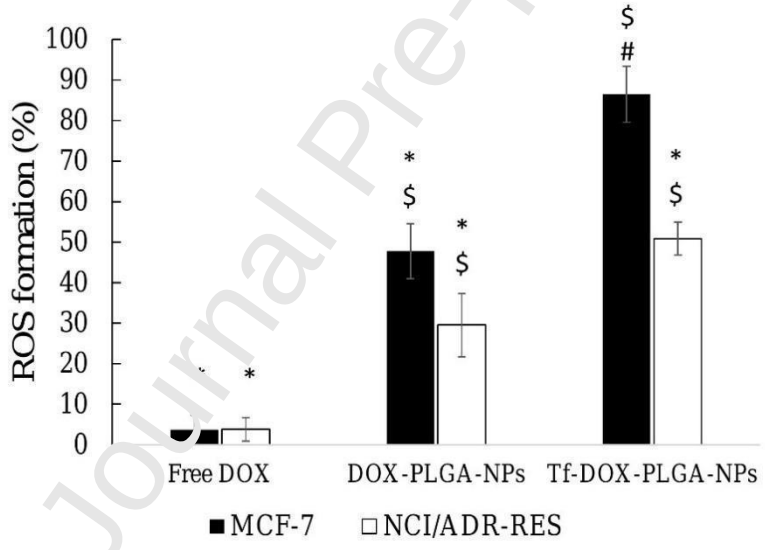

Figure 10. Effect of free and loaded DOX on ROS levels in MCF-7 and NCI/ADR-RES cells measured by flow cytometry after 24 h treatment. Untreated cells were taken as control. Statistical analysis was performed using ANOVA followed by Tukey's multiple comparison test. * is different from the control, # is different from DOX-PLGA-NPs and $ is different from free DOX ($p < 0.05$). Values are mean ± SD, n = 3.

4 DISCUSSION

DOX has been widely used as anticancer treatment for over 50 years and is effective against lymphoma, sarcoma, leukemia, lung, brains, ovarian and breast cancer; however, the

major dose-limiting toxicity are acute neutropenia and cumulative cardiomyopathy, which can advance into congestive heart failure [32–34]. The designed Tf-DOX-PLGA-NPs comprise three distinct functional components: the surfactant 77KS, poloxamer and Tf. Our previous data demonstrated that Tf-conjugated DOX-loaded PLGA-NPs were capable to promote the drug release in a pH-dependent manner, achieving higher rates in acidic environments, as found i.e. in the tumor tissue [13]. Therefore, our previous results encouraged us to investigate whether the synergistic association of 77KS, Tf and poloxamer could potentialize DOX antiproliferative activity against MDR cells. The studies presented here considered especially the comparative impact of Tf-DOX-PLGA-NPs toward MDR NCI/ADR-RES cancer cells and DOX-sensitive cancer cells. NCI/ADR-RES cells display multiple mechanisms to trigger and maintain the drug resistance, such as overexpression of genes and proteins involved in drug extrusion, inactivation and efficacy, as well as architectural and functional extracellular matrix reorganization forming a dense cellular structure that limit drug diffusion into cells [24]. Being the Pgp pump efflux the most prevalent and important mechanism of drug resistance, some works have focused on modulating or inhibiting the Pgp activity as an attempt to circumvent the MDR effect [35–38]. Poloxamer deserves to be highlighted as cytotoxicity enhancers in sensitive cancer cells [13,22,39], tumor sensitizers in MDR cells [4–6], and colloidal suspension stabilizers [22,40]. Likewise, the target ligand Tf could increase the DOX effectiveness, alleviating MDR [9].

Once a nanomaterial enters the human body, it is exposed to environments which can alter its surface composition forming a layer of adsorbed proteins. The protein corona formation can affect the efficacy of nanomedicines since the internalization and drug release can be impacted [17]. As a further characterization study of the NPs, we exposed them to protein-containing media in order to verify the possible protein corona formation. No significant increase in the mean particle size was observed, which suggest that the NP surface is not modified by adsorption of biomolecules from the biological media. It is also worth mentioning that the lack of NP-protein interactions with consequent protein corona formation might be also attributed to the presence of poloxamer as a stabilizer in the colloidal formulations [41]. Moreover, this data positively suggests that the Tf-NPs surface conjugation has not been undone and Tf was not replaced by albumin or other protein [42].

The likely journey of the NPs through the body is to reach the tumor region and/or tumor cell by passive targeting via leaky tumor vasculature and reduced lymphatic drainage, by pH-stimulus response effect and/or by active targeting via specific ligand [20]. In this context, our previous study showed the pH-dependent DOX release from both DOX-PLGA-

NPs and Tf-DOX-PLGA-NPs, as well as the pH-dependent membrane lytic activity of the NPs, which mean that higher drug concentration might be found in the acidic tumor region, and in the intracellular compartments after NP uptake and subsequent endosome destabilization [13]. Moreover, taking into account the pronounced greater number of TfR in cancerous cells [8], our cytotoxicity results were in the sense to confirm the enhancing on cell-specificity of DOX when loaded in Tf-modified nanostructures, as also achieved in other studies [14,16,43–45]. Here, we showed the cell viability reducing on three different tumor cell lines as DOX concentration and incubation time increased, by both MTT and NRU viability assays. Tf decoration of the surface of DOX-loaded NPs enhanced the drug antiproliferative activity. This improved cytotoxicity can be especially attributed to the NP targetability, as targeting allows for enhanced drug cellular uptake, and improved cellular targeting in order to effectively deliver therapeutic compounds to disease site [46].

After the initial screening on different tumor cells, further experiments were carried out comparatively between MCF-7, as a model of DOX-sensitive cell line, and NCI/ADR-RES, as a model of MDR cells, using the MTT viability endpoint. Free DOX and DOX-loaded NPs showed an expressive toxicity on the sensitive cells, which was expected, especially by the Tf-decorated NPs. On the other hand, the DOX loaded NPs were markedly superior in terms of cytotoxic activity in comparison to DOX solution on the MDR cells. This distinction was already significative at 24 h incubation, but enhanced in a time-dependent manner. The weak potency of unloaded DOX is probably due to its removal from cells, following its uptake, via the ATP-dependent efflux transporters that are overexpressed in MDR cell lines [47]. Most importantly, the outstanding antiproliferative activity of the Tf-conjugated NPs highlights the synergistic role of the biomarker Tf and the sensitizer poloxamer in the improvement of chemotherapy ($p < 0.05$). Likewise, it was previously reported that poloxamer-Tf-engineered NPs appeared to have a better application in MDR tumors by reducing the cell respiration rate, then enhancing the sensitivity to antitumor agents [48,49]. Additionally, it is worth mentioning that different studies have reported an upregulation in expression of the TfR on metastatic and drug resistant tumors [50,51], which might explain the higher antiproliferative potential of Tf-DOX-PLGA-NPs with respected to MDR cells. An important mechanism underlying MDR is the impaired delivery of antitumor drugs to cancer cells [52], and the active targeting of tumor cells with Tf has been shown to have the ability to overcome this resistance mechanism. Indeed, it has been shown that Tf-targeted nanosystems enhanced delivery of chemotherapeutics into MDR tumor cells, reversing at some extent their drug resistance. This behavior might be attributed to an increase of circulation time and internalization via Tf-

mediated mechanisms, with the cell unable to recognize the drug in its encapsulated state, which consequently results in a higher drug accumulation into the cell [9, 53-55].

The results of the cellular uptake studies showed the effective Tf-DOX-PLGA-NPs internalization in a time-dependent manner, in both MCF-7 and NCI/ADR-RES cells. In agreement with the flow cytometry experiments, the enhanced cellular uptake of Tf-inspired NPs compared to free DOX was further confirmed by fluorescence microscopy, via staining the nucleus and cytoplasm. DOX was mainly accumulated in the nucleus of MCF-7 cells, thereby increasing the fluorescence intensity. For NCI/ADR-RES cells, weak DOX signal was detected in the free drug treated group, suggesting that Pgp-mediated efflux does work. Tf-DOX-PLGA-NPs were internalized by MDR cells to a lesser extent than in MCF-7 cells, but no less efficient, and DOX was localized into the cytoplasm and nucleus, suggestive of inhibition or bypassing Pgp transporter. This behavior might explain the positive correlation between the increased cell uptake and higher antiproliferative activity of Tf-decorated-NPs in resistant cells. Once accumulated into the nucleus of MDR cells, the drug becomes able to exert its therapeutic effects such as cell growth inhibition and, ultimately, cell death [56]. In our previous study, we demonstrated the controlled membranolytic activity of Tf-modified NPs in acidic medium simulating the endo-lysosomal compartments [13]. Linking these data, DOX encapsulated in these NPs could enhance intracellular accumulation of the drug, achieving a gradual release from the endosomes, thus entering the nucleus, which finally result in the outstanding greater cytotoxicity of DOX in the MDR cells. Similar behavior was observed by He et al., which demonstrated a lysosomotropic delivery pathway of Tf-NPs [9].

The TfR is an essential transmembrane protein involved in iron uptake and the regulation of cell growth, being overexpressed on cancer cells. The iron endocytosis occurs via clathrin-coated pits, which is delivered from endosomes to the cytosol [57]. Regarding the nanomaterials, they were reported to be uptake by clathrin- and caveolin-mediated endocytosis, phagocytosis and/or macropinocytosis [58]. Therefore, the uptake mechanism of the NPs was studied using some endocytic inhibitors. A remarkable reduced number of NPs was internalized in both cell lines when incubated at 4°C, indicating the energy dependence for cell uptake. Endocytosis as well as macropinocytosis are stated as active transport processes of substances, in which energy is required [59]. Simultaneously, the entry of Tf-DOX-PLGA-NPs was partially inhibited when the cells were previously exposed to an excess amount of Tf, suggesting that the receptor-mediated and energy dependence might be the multipathway for Tf-DOX-PLGA-NPs internalization into NCI/ADR-RES cells. The specificity of Tf-NPs binding to Tf receptors and the subsequently higher cytotoxicity was

reported in prostate and glioblastoma cancer cells [10,29]. Likewise, by targeting the TfR through its endocytic mechanisms, different studies have shown Tf-conjugated nanocarriers highly effective in reversing MDR [53,54]. An undefined TfR-independent mechanism has also been suggested, since excess of Tf did not prevent Tf-DOX conjugate or Tf-modified NPs uptake in diverse cancer cells [60,61].

Concerning the mechanisms underlying the greater antitumor activity of the NPs, it has been previously shown that Tf-inspired NPs induced not only drug-sensitive cell but also MDR cell death through apoptosis [49]. Here, Tf-DOX-PLGA-NPs elicited a substantial increase in the amount of apoptotic MDR cells and consequently the percentage of normal cells was lower than in other groups, confirming their outstanding results on the cytotoxicity studies. Moreover, Tf-DOX-PLGA-NPs inhibits cell growth and proliferation by its effect on the cell cycle, arresting the MDR cells in S and sub-G1 phases. The sub-G1 phase is also called apoptotic peak where the DNA content is fragmented [62]. Therefore, our results showed that Tf-inspired NPs were able to induce a greater apoptotic response in MDR cells than the other treatments, which is in accordance with apoptosis experiments using Annexin V/PI. It is known that DOX might be available in the nucleus to lead the cells to apoptosis, once this drug acts through intercalation into DNA [63]. Thus, the overall findings allow us to suggest that Tf-DOX-PLGA-NPs deliver the drug into MDR cells, becoming ready to escape from endo-lysosomal compartments via pH-dependent membrane-lytic activity of the 77KS, finally reaching the nucleus. Concerning free DOX and DOX-PLGA-NPs, we observed that both of them arrested the sensitive and MDR cells in the G2/M phase. This is in a good agreement with studies published earlier, which demonstrated the same behavior for free DOX on progression of sensitive and resistant cancer cells [30,49,64]. Besides the DOX role on apoptosis and cell cycle progress, it is also important to consider the topoisomerase II inhibition, DNA strand break, and ROS formation as mechanisms of action. A significant increase in ROS levels in the sensitive and MDR cells was observed after treatment with Tf-inspired NPs, in contrast to the free DOX, which displayed only a slight enhancement independent of the cell line. The involvement of ROS in the activation of the apoptotic signaling pathway configure one more mechanism by which Tf-DOX-PLGA-NPs promotes the tumor cells death and confirm its highly potent antiproliferative activity. Increased ROS generation in tumor cells might induces oxidative stress, loss of cytochrome c, activation of caspase cascade and lipid peroxidation [31]. Finally, it is worth linking the enhance of ROS formation and apoptosis induction to the synergistic role of poloxamer on the Tf-targeted NPs, as also previously reported [5,49].

The sustained release can be considered the main advantage of the NPs, once the drug encapsulated is not exposed to the cell membrane associated efflux pump transporters. Pgp is reported to be the major efflux pump on NCI/ADR-RES cells, promoting exocytosis and drug resistance [24]. Indeed, the intracellular drug retention experiment suggests that the enhancing in DOX retention by cells treated with Tf-modified NPs can be ascribed to the uptake and internalization behavior of this NPs promoted by the Tf-TfR interaction, unlike the unmodified NPs and especially the free drug. This difference between the uptake pathway probably influences the intracellular retention as wells as its ability to mitigate the drug efflux [9, 29].

5 CONCLUSIONS

In this study, it was evidenced that our pH-sensitive Tf-decorated PLGA-NPs are effective to deliver DOX to resistant tumor cells by pH-stimulus and Tf-targetability, also alleviating MDR by the synergistic action of Tf and poloxamer. The correlation between cell growth inhibition and the higher apoptotic rate and ROS formation promoted by Tf-NPs was also observed. Apoptotic changes caused by Tf-decorated NPs in MDR cells were also accompanied by cell cycle arresting at sub-G1 and S phases. Moreover, Tf-decorated NPs were internalized in a higher extent into P-gp over-expressing NCI/ADR-RES cells than free DOX and nontargeted counterparts, supporting the observed greater cell killing ability of DOX release from targeted NPs with respect to MDR cells. Overall, the results evidenced the feasibility of *in vitro* approaches to prove the effectiveness of the nanocarrier platform proposed here, reinforcing the optimism about the use of DOX in antineoplastic therapy and MDR reversal. However, additional evaluations using 3D *in vitro* cell models along with studies under *in vivo* conditions must be conducted to confirm this evidence.

ACKNOWLEDGEMENTS

This research was supported by Projects 447548/2014-0 and 401069/2014-1 of the Conselho Nacional de Desenvolvimento Científico e Tecnológico (CNPq - Brazil). L.E.S thanks the Coordenação de Aperfeiçoamento de Pessoal de Nível Superior (CAPES - Brazil) for the PhD fellowship at Universidade Federal de Santa Maria and CNPq for the PhD internship at Universitat de Barcelona (Grant 204255/2018-0). D.R.N-L. thanks CNPq (Grant 150920/2018-0) and CAPES (Grant 88887.374254/2019-00) for the Postdoctoral grants.

CONFLICTS OF INTEREST

The authors declare no conflict of interest.

REFERENCES

[1] Carvalho, C.; Santos, R.; Cardoso, S.; Correia, S.; Oliveira, P.; Santos, M.; Moreira, P. Doxorubicin: The Good, the Bad and the Ugly Effect. Curr. Med. Chem. 2009, 16, 3267–3285, doi:10.2174/092986709788803312.

[2] Minko, T.; Rodriguez-Rodriguez, L.; Pozharov, V. Nanotechnology approaches for personalized treatment of multidrug resistant cancers. Adv. Drug Deliv. Rev. 2013, 65, 1880–1895, doi:10.1016/j.addr.2013.09.017.

[3] Garcia-Mayea, Y.; Mir, C.; Masson, F.; Paciucci, R.; LLeonart, M.E. Insights into new mechanisms and models of cancer stem cell multidrug resistance. Semin. Cancer Biol. 2020, 60, 166–180, doi:10.1016/j.semcancer.2019.07.022.

[4] Batrakova, E. V.; Li, S.; Brynskikh, A.M.; Sharma, A.K.; Li, Y.; Boska, M.; Gong, N.; Mosley, R.L.; Alakhov, V.Y.; Gendelman, H.E.; et al. Effects of pluronic and doxorubicin on drug uptake, cellular metabolism, apoptosis and tumor inhibition in animal models of MDR cancers. J. Control. Release 2010, 143, 290–301, doi:10.1016/j.jconrel.2010.01.004.

[5] Alakhova, D.Y.; Rapoport, N.Y.; Batrakova, E. V.; Timoshin, A.A.; Li, S.; Nicholls, D.; Alakhov, V.Y.; Kabanov, A. V. Differential metabolic responses to pluronic in MDR and non-MDR cells: A novel pathway for chemosensitization of drug resistant cancers. J. Control. Release 2010, 142, 89–100, doi:10.1016/j.jconrel.2009.09.026.

[6] Cheng, X.; Lv, X.; Xu, J.; Zheng, Y.; Wang, X.; Tang, R. Pluronic micelles with suppressing doxorubicin efflux and detoxification for efficiently reversing breast cancer resistance. Eur. J. Pharm. Sci. 2020, 146, 105275, doi:10.1016/j.ejps.2020.105275.

[7] Shen, Z.; Nieh, M.P.; Li, Y. Decorating nanoparticle surface for targeted drug delivery: Opportunities and challenges. Polymers (Basel). 2016, 8, 1–18, doi:10.3390/polym8030083.

[8] Gomme, P.T.; McCann, K.B. Transferrin: Structure, function and potential therapeutic actions. Drug Discov. Today 2005, 10, 267–273, doi:10.1016/S1359-6446(04)03333-1.

[9] He, Y.J.; Xing, L.; Cui, P.F.; Zhang, J.L.; Zhu, Y.; Qiao, J. Bin; Lyu, J.Y.; Zhang, M.; Luo, C.Q.; Zhou, Y.X.; et al. Transferrin-inspired vehicles based on pH-responsive coordination bond to combat multidrug-resistant breast cancer. Biomaterials 2017, 113, 266–278, doi:10.1016/j.biomaterials.2016.11.001.

[10] Jhaveri, A.; Deshpande, P.; Pattni, B.; Torchilin, V. Transferrin-targeted, resveratrol-loaded liposomes for the treatment of glioblastoma. J. Control. Release 2018, 277, 89–101, doi:10.1016/j.jconrel.2018.03.006.

[11] Sharma, S.; Parmar, A.; Kori, S.; Sandhir, R. PLGA-based nanoparticles: A new paradigm in biomedical applications. TrAC - Trends Anal. Chem. 2016, 80, 30–40,

doi:10.1016/j.trac.2015.06.014.

[12] Shen, X.; Li, T.; Xie, X.; Feng, Y.; Chen, Z.; Yang, H.; Wu, C.; Deng, S.; Liu, Y. PLGA-Based Drug Delivery Systems for Remotely Triggered Cancer Therapeutic and Diagnostic Applications. Front. Bioeng. Biotechnol. 2020, 8, 1–19, doi:10.3389/fbioe.2020.00381.

[13] Scheeren, L.E.; Nogueira-Librelotto, D.R.; Macedo, L.B.; de Vargas, J.M.; Mitjans, M.; Vinardell, M.P.; Rolim, C.M.B. Transferrin-conjugated doxorubicin-loaded PLGA nanoparticles with pH-responsive behavior: a synergistic approach for cancer therapy. J. Nanoparticle Res. 2020, 22, doi:10.1007/s11051-020-04798-7.

[14] Zhang, X.; Li, J.; Yan, M. Targeted hepatocellular carcinoma therapy: transferrin modified, self-assembled polymeric nanomedicine for co-delivery of cisplatin and doxorubicin. Drug Dev. Ind. Pharm. 2016, 42, 1590–1598, doi:10.3109/03639045.2016.1160103.

[15] Cui, Y.; Xu, Q.; Chow, P.K.H.; Wang, D.; Wang, C.H. Transferrin-conjugated magnetic silica PLGA nanoparticles loaded with doxorubicin and paclitaxel for brain glioma treatment. Biomaterials 2013, 34, 8511–8520, doi:10.1016/j.biomaterials.2013.07.075.

[16] Guo, Y.; Wang, L.; Lv, P.; Zhang, P. Transferrin-conjugated doxorubicin-loaded lipid-coated nanoparticles for the targeting and therapy of lung cancer. Oncol. Lett. 2015, 9, 1065–1072, doi:10.3892/ol.2014.2840.

[17] Bregoli, L.; Movia, D.; Gavigan-Imedio, J.D.; Lysaght, J.; Reynolds, J.; Prina-Mello, A. Nanomedicine applied to translational oncology: A future perspective on cancer treatment. Nanomedicine Nanotechnology, Biol. Med. 2016, 12, 81–103, doi:10.1016/j.nano.2015.08.006.

[18] Bidkar, A.P.; Sanpui, P.; Ghosh, S.S. Transferrin-Conjugated Red Blood Cell Membrane-Coated Poly(lactic- co-glycolic acid) Nanoparticles for the Delivery of Doxorubicin and Methylene Blue. ACS Appl. Nano Mater. 2020, 3, 3807–3819, doi:10.1021/acsanm.0c00502.

[19] Zhang, X.; Zhao, L.; Zhai, G.; Ji, J.; Liu, A. Multifunctional polyethylene glycol (PEG)-Poly (Lactic-Co-Glycolic Acid) (PLGA)-based nanoparticles loading doxorubicin and tetrahydrocurcumin for combined chemoradiotherapy of glioma. Med. Sci. Monit. 2019, 25, 9737–9751, doi:10.12659/MSM.918899.

[20] Vives, M.A.; Infante, M.R.; Garcia, E.; Selve, C.; Maugras, M.; Vinardell, M.P. Erythrocyte hemolysis and shape changes induced by new lysine-derivate surfactants. Chem. Biol. Interact. 1999, 118, 1–18, doi:10.1016/S0009-2797(98)00111-2.

[21] Nogueira, D.R.; Carmen Morán, M.; Mitjans, M.; Martínez, V.; Pérez, L.; Pilar Vinardell, M. New cationic nanovesicular systems containing lysine-based surfactants for topical administration: Toxicity assessment using representative skin cell lines. Eur. J. Pharm. Biopharm. 2013, 83, 33–43, doi:10.1016/j.ejpb.2012.09.007.

[22] Scheeren, L.E.; Nogueira, D.R.; Macedo, L.B.; Vinardell, M.; Mitjans, M.; Infante, M.; Rolim, C.M.B. PEGylated and poloxamer-modified chitosan nanoparticles

incorporating a lysine-based surfactant for pH-triggered doxorubicin release. Colloids Surfaces B Biointerfaces 2016, 138, doi:10.1016/j.colsurfb.2015.11.049.

[23] Fessi, H.; Puisieux, F.; Devissaguet, J.P.; Ammoury, N.; Benita, S. Nanocapsule formation by interfacial polymer deposition following solvent displacement. Int. J. Pharm. 1989, 55, 1–4, doi:10.1016/0378-5173(89)90281-0.

[24] Vert, A.; Castro, J.; Ribó, M.; Vilanova, M.; Benito, A. Transcriptional profiling of NCI/ADR-RES cells unveils a complex network of signaling pathways and molecular mechanisms of drug resistance. Onco. Targets. Ther. 2018, 11, 221–237, doi:10.2147/OTT.S154378.

[25] Mosmann, T. Rapid colorimetric assay for cellular growth and survival: Application to proliferation and cytotoxicity assays. J. Immunol. Methods 1983, 65, 55–63, doi:10.1016/0022-1759(83)90303-4.

[26] Borenfreund, E.; Puerner, J.A. Toxicity determined in vitro by morphological alterations and neutral red absorption. Toxicol. Lett. 1985, 24, 119.

[27] Nogueira-Librelotto, D.R.; Scheeren, L.E.; Vinardell, M.P.; Mitjans, M.; Rolim, C.M.B. Chitosan-tripolyphosphate nanoparticles functionalized with a pH-responsive amphiphile improved the in vitro antineoplastic effects of doxorubicin. Colloids Surfaces B Biointerfaces 2016, 147, doi:10.1016/j.colsurfb.2016.08.014.

[28] Nogueira, D.R.; Tavano, L.; Mitjans, M.; Pérez, L.; Infante, M.R.; Vinardell, M.P. In vitro antitumor activity of methotrexate via pH-sensitive chitosan nanoparticles. Biomaterials 2013, 34, 2758–2772, doi:10.1016/j.biomaterials.2013.01.005.

[29] Sahoo S.K. and Labhasetwar V. Enhanced antiproliferative activity of transferrin-conjugated paclitaxel-loaded nanoparticles is mediated via sustained intracellular drug retention. Activity of. Mol. Pharm. 2005, 2, 373–383. doi: 10.1021/mp050032z.

[30] Nogueira-Librelotto, D.R., Scheeren, L.E.; Macedo, L.B.; Vinardell, M.P.; Rolim, C.M.B. pH-Sensitive chitosan-tripolyphosphate nanoparticles increase doxorubicin-induced growth inhibition of cervical HeLa tumor cells by apoptosis and cell cycle modulation. Colloids Surfaces B Biointerfaces 2020, 190, 110897, doi:10.1016/j.colsurfb.2020.110897.

[31] Yuan, Y.; Cai, T.; Callaghan, R.; Li, Q.; Huang, Y.; Wang, B.; Huang, Q.; Du, M.; Ma, Q.; Chiba, P.; et al. Psoralen-loaded lipid-polymer hybrid nanoparticles enhance doxorubicin efficacy in multidrug-resistant HepG2 cells. Int. J. Nanomedicine 2019, 14, 2207–2218, doi:10.2147/IJN.S189924.

[32] Pereverzeva, E.; Treschalin, I.; Treschalin, M.; Arantseva, D.; Ermolenko, Y.; Kumskova, N.; Maksimenko, O.; Balabanyan, V.; Kreuter, J.; Gelperina, S. Toxicological study of doxorubicin-loaded PLGA nanoparticles for the treatment of glioblastoma. Int. J. Pharm. 2019, 554, 161–178, doi:10.1016/j.ijpharm.2018.11.014.

[33] Alibolandi, M.; Sadeghi, F.; Abnous, K.; Atyabi, F.; Ramezani, M.; Hadizadeh, F. The chemotherapeutic potential of doxorubicin-loaded PEG-b-PLGA nanopolymersomes in mouse breast cancer model. Eur. J. Pharm. Biopharm. 2015, 94, 521–531, doi:10.1016/j.ejpb.2015.07.005.

[34] Vejpongsa, P.; Yeh, E.T.H. Prevention of anthracycline-induced cardiotoxicity: Challenges and opportunities. J. Am. Coll. Cardiol. 2014, 64, 938–945, doi:10.1016/j.jacc.2014.06.1167.

[35] Batrakova, E. V.; Kabanov, A. V. Pluronic block copolymers: Evolution of drug delivery concept from inert nanocarriers to biological response modifiers. J. Control. Release 2008, 130, 98–106, doi:10.1016/j.jconrel.2008.04.013.

[36] Batrakova, E. V.; Li, S.; Elmquist, W.F.; Miller, D.W.; Alakhov, V.Y.; Kabanov, A. V. Mechanism of sensitization of MDR cancer cells by Pluronic block copolymers: Selective energy depletion. Br. J. Cancer 2001, 85, 1987–1997, doi:10.1054/bjoc.2001.2165.

[37] Kabanov, A. V.; Batrakova, E. V.; Alakhov, V.Y. Pluronic® block copolymers for overcoming drug resistance in cancer. Adv. Drug Deliv. Rev. 2002, 54, 759–779, doi:10.1016/S0169-409X(02)00047-9.

[38] Moloughney, J. G.; Weisleder, N. Poloxamer 188 (P188) as a Membrane Resealing Reagent in Biomedical Applications. Recent Pat. Biotechnol. 2013, 6, 200–211, doi:10.2174/1872208311206030200.

[39] Gelperina, S.; Maksimenko, O.; Khalansky, A.; Vanchugova, L.; Shipulo, E.; Abbasova, K.; Berdiev, R.; Wohlfart, S.; Chepurnova, N.; Kreuter, J. Drug delivery to the brain using surfactant-coated poly(lactide-co-glycolide) nanoparticles: Influence of the formulation parameters. Eur. J. Pharm. Biopharm. 2010, 74, 157–163, doi:10.1016/j.ejpb.2009.09.003.

[40] Guimarães, P.P.G.; Oliveira, S.N.; De Castro Rodrigues, G.; Gontijo, S.M.L.; Lula, I.S.; Cortés, M.E.; Denadaie, Â.M.L.; Sinisterra, R.D. Development of sulfadiazine-decorated PLGA nanoparticles loaded with 5-fluorouracil and cell viability. Molecules 2015, 20, 879–899, doi:10.3390/molecules20010879.

[41] Shubhra, Q.T.H.; Tóth, J.; Gyenis, J.; Feczkó, T. Surface modification of HSA containing magnetic PLGA nanoparticles by poloxamer to decrease plasma protein adsorption. Colloids Surfaces B Biointerfaces 2014, 122, 529–536, doi:10.1016/j.colsurfb.2014.07.025.

[42] Pitek, A.S.; O'Connell, D.; Mahon, E.; Monopoli, M.P.; Francesca Baldelli, F.; Dawson, K.A. Transferrin coated nanoparticles: Study of the bionano interface in human plasma. PLoS One 2012, 7, doi:10.1371/journal.pone.0040685.

[43] Szwed, M.; Matusiak, A.; Laroche-Clary, A.; Robert, J.; Marszalek, I.; Jozwiak, Z. Transferrin as a drug carrier: Cytotoxicity, cellular uptake and transport kinetics of doxorubicin transferrin conjugate in the human leukemia cells. Toxicol. Vitr. 2014, 28, 187–197, doi:10.1016/j.tiv.2013.09.013.

[44] Tavano, L.; Muzzalupo, R.; Mauro, L.; Pellegrino, M.; Andò, S.; Picci, N. Transferrin-conjugated Pluronic niosomes as a new drug delivery system for anticancer therapy. Langmuir 2013, 29, 12638–12646, doi:10.1021/la4021383.

[45] Sriraman, S.K.; Salzano, G.; Sarisozen, C.; Torchilin, V. Anti-cancer activity of doxorubicin-loaded liposomes co-modified with transferrin and folic acid. Eur. J.

Pharm. Biopharm. 2016, 105, 40–49, doi:10.1016/j.ejpb.2016.05.023.

[46] Kim, S.; Saha, K.; Kim, C.; Rotello, V. The role of surface functionality in determining nanoparticle cytotoxicity. Acc. Chem. Res. 2013, 46, 681–691, doi: 10.1021/ar3000647.

[47] Cox, J.; Weinman, S. Mechanisms of doxorubicin resistance in hepatocellular carcinoma. Hepatic Oncol. 2016, 3, 57–59, doi: 10.2217/hep.15.41.

[48] Zhu, B.; Zhang, H.; Yu, L. Novel transferrin modified and doxorubicin loaded Pluronic 85/lipid-polymeric nanoparticles for the treatment of leukemia: In vitro and in vivo therapeutic effect evaluation. Biomed. Pharmacother. 2017, 86, 547–554, doi:10.1016/j.biopha.2016.11.121.

[49] Soe, Z.C.; Kwon, J.B.; Thapa, R.K.; Ou, W.; Nguyen, H.T.; Gautam, M.; Oh, K.T.; Choi, H.G.; Ku, S.K.; Yong, C.S.; et al. Transferrin-conjugated polymeric nanoparticle for receptor-mediated delivery of doxorubicin in doxorubicin-resistant breast cancer cells. Pharmaceutics 2019, 11, 1–17, doi:10.3390/pharmaceutics11020063.

[50] Ryschich, E.; Huszty, G.; Knaebel, H.P.; Hartel, M.; Büchler, M.W.; Schmidt, J. Transferrin receptor is a marker of malignant phenotype in human pancreatic cancer and in neuroendocrine carcinoma of the pancreas. Eur. J. Cancer 2004, 40, 1418–1422, doi: 10.1016/j.ejca.2004.01.036.

[51] Calzolari, A.; Oliviero, I.; Deaglio, S.; Mariani, G.; Biffoni, M.; Sposi, N.; Malavasi, F.; Peschle, C.; Testa, U. Transferrin receptor 2 is frequently expressed in human cancer cell lines. Blood Cells Mol. Dis. 2007, 39, 82–91, doi: 10.1016/j.bcmd.2007.02.003.

[52] Gottesman, M.M.; Fojo, T.; Bates, S.E. Multidrug resistance in cancer: role of ATP-dependent transporters. Nat. Rev. Cancer 2002, 2, 48–58. doi: 10.1038/nrc706.

[53] Chiu, S.-J.; Liu, S.; Perrotti, D.; Marcucci, G.; Lee, R. Efficient delivery of a Bcl-2-specific antisense oligodeoxyribonucleotide (G3139) via transferrin receptor-targeted liposomes. J. Control. Release 2006, 112, 199–207, doi: 10.1016/j.jconrel.2006.02.011.

[54] Wu, J.; Lu, Y.; Lee, A.; Pan, X.; Yang, X.; Zhao, X.; Lee, R. Reversal of multidrug resistance by transferrin-conjugated liposomes coencapsulating doxorubicin and verapamil. J. Pharm. Pharm. Sci. 2007, 10, 350–357.

[55] Qin, M.; Lee, Y.-E. K.; Ray, A.; Kopelman, R. Overcoming cancer multidrug resistance by codelivery of doxorubicin and verapamil with hydrogel nanoparticles. Macromol. Biosci. 2014, 14, 1106-1115, doi: 10.1002/mabi.201400035.

[56] Wang, F.; Jiang, X.; Yang, D.C.; Elliott, R.L.; Head, J.F. Doxorubicin–gallium–transferrin conjugate overcomes multidrug resistance: evidence for drug accumulation in the nucleus of drug resistant MCF-7/ADR cells. Anticancer Res. 2000, 20, 799–808.

[57] Daniels, T.R.; Delgado, T.; Rodriguez, J.A.; Helguera, G.; Penichet, M.L. The transferrin receptor part I: Biology and targeting with cytotoxic antibodies for the treatment of cancer. Clin. Immunol. 2006, 121, 144–158, doi:10.1016/j.clim.2006.06.010.

[58] Iversen, T.G.; Skotland, T.; Sandvig, K. Endocytosis and intracellular transport of nanoparticles: Present knowledge and need for future studies. Nano Today 2011, 6, 176–185, doi:10.1016/j.nantod.2011.02.003.

[59] Xie, Q.; Deng, W.; Yuan, X.; Wang, H.; Ma, Z.; Wu, B.; Zhang, X. Selenium-functionalized liposomes for systemic delivery of doxorubicin with enhanced pharmacokinetics and anticancer effect. Eur. J. Pharm. Biopharm. 2018, 122, 87–95, doi:10.1016/j.ejpb.2017.10.010.

[60] Lai, B.T.; Gao, J.P.; Lanks, K.W. Mechanism of action and spectrum of cell lines sensitive to a doxorubicin-transferrin conjugate. Cancer Chemother. Pharmacol. 1997, 41, 155–160, doi:10.1007/s002800050722.

[61] Jin, S.; Zhang, Y.; Yu, C.; Wang, G.; Zhang, Z.; Li, N.; Na, Y. Transferrin-modified PLGA nanoparticles significantly increase the cytotoxicity of paclitaxel in bladder cancer cells by increasing intracellular retention. J. Nanoparticle Res. 2014, 16, doi:10.1007/s11051-014-2639-0.

[62] Meena, R.; Kesari, K.K.; Rani, M.; Paulraj, R. Effects of hydroxyapatite nanoparticles on proliferation and apoptosis of human breast cancer cells (MCF-7). J. Nanoparticle Res. 2012, 14, doi:10.1007/s11051-011-0712-5.

[63] Panyam, J.; Labhasetwar, V. Sustained cytoplasmic delivery of drugs with intracellular receptors using biodegradable nanoparticles. Mol. Pharm. 2004, 1, 77–84, doi:10.1021/mp034002c.

[64] Misra, R.; Sahoo, S.K. Intracellular trafficking of nuclear localization signal conjugated nanoparticles for cancer therapy. Eur. J. Pharm. Sci. 2010, 39, 152–163, doi:10.1016/j.ejps.2009.11.010.

Declaration of interests

☒ The authors declare that they have no known competing financial interests or personal relationships that could have appeared to influence the work reported in this paper.

☐The authors declare the following financial interests/personal relationships which may be considered as potential competing interests:

Highlights

- Transferrin-decorated pH-sensitive PLGA-NPs increased DOX specificity in tumor cells;
- Transferrin-decorated NPs (Tf-NPs) were mostly effective against resistant cells;
- Poloxamer and the pH-responsive adjuvant 77KS act synergistically with transferrin;
- Targeted Tf-NPs were greater internalized into sensitive and MDR tumor cells;
- Apoptotic effects, cell cycle arrest and ROS formation support the cytotoxicity.